



# Effects of crystal orientation on bendability of aluminum alloy sheet

Shingo Ikawa<sup>a,b,\*</sup>, Mineo Asano<sup>a</sup>, Mitsutoshi Kuroda<sup>b</sup>, Kengo Yoshida<sup>b</sup>

<sup>a</sup> R&D Center, Sumitomo Light Metal Industries, Ltd., 3-1-12 Chitose, Minato-ku, Nagoya, Aichi 455-8670, Japan

<sup>b</sup> Graduate School of Science and Engineering, Yamagata University, 4-3-16 Jonan, Yonezawa, Yamagata 992-8510, Japan

## ARTICLE INFO

### Article history:

Received 9 November 2010

Received in revised form 4 January 2011

Accepted 18 January 2011

Available online 22 January 2011

### Keywords:

Shear band  
Crystal plasticity  
Single crystal  
FEM simulation  
Texture

## ABSTRACT

We investigated the effects of crystal orientation on the bendability of aluminum alloy sheets by experiments using single crystal specimens and finite element analysis using a crystal plasticity model. In the experimental investigation, single crystal specimens having cube and Goss orientations were made from a coarse-grained Al–Mg–Si alloy sheet. The cube single crystal specimens have shown an excellent bendability regardless of the bending direction. Meanwhile, the bendability of the Goss single crystal specimens strongly depended on the bending direction. The finite element analysis results are remarkably consistent with the experimental results.

© 2011 Elsevier B.V. All rights reserved.

## 1. Introduction

The reduction of the greenhouse gas, such as CO<sub>2</sub>, is a critical problem for global environmental protection. As a structural engineering approach, lightening the transportation vehicle by applying lightweight metals to their structural assemblies is a promising and efficient strategy. Furthermore, demands for downsizing of the structural members and sharpening exterior parts are also rapidly increasing. This situation has raised the need for the application of aluminum alloy sheets with a higher formability that can be easily formed into complex shaped parts or members. The improvement in *bendability* is one of the most important key factors to expand the applicability of aluminum alloy sheets to various types of structural members, which demand a high strength but are lightweight.

The limit to the ductility of metal sheets is usually set by the localized deformation in the form of the *macroscopic shear band* (*macro-shear band*) that suddenly appears at a certain stage during plastic deformation. In the case of bending, the macro-shear band develops from the surface then into the inside of the sheet thickness, and finally leading to breaking of the material. It has been reported that the bendability, which is limited by the macro-shear band formation, depends on amounts of solute atoms [1,2], population of the second phase particles [3], and crystal orientations (or texture) [4,5]. In Refs. [4,5], a pure bending problem of the

aluminum alloy sheets with typical texture components (copper, brass, S, cube and Goss) was analyzed by a finite element method that employed the crystal plasticity model [6]. It was shown that the crystal orientations have a significant influence on the bendability, and especially the cube texture produces a remarkably enhanced bendability.

It is important to confirm these findings by an experimental investigation. However, it is difficult to extract the effect of one specific crystal orientation from a test result for an industrial polycrystalline material with a complex crystallographic texture that consists of various components developed during rolling and subsequent annealing processes.

In the present study, we conducted bending tests on single crystal specimens to experimentally verify the effects of the crystal orientations on the bendability. The single crystal specimens were made from an Al–Mg–Si alloy sheet with large-sized crystal grains. The experimental results are compared to the computational results from finite element analysis using a crystal plasticity constitutive model.

## 2. Experimental

### 2.1. Experimental procedure

Crystal grains in an A6061-T4 alloy sheet with sheet thickness of 1.0 mm were grown in the range of 20–30 mm at a cooling speed about 293 K/s after a 1.8 ks heat-treatment at 823 K. Fig. 1(a) shows the surface of the A6061-T4 alloy sheet with macroetching. A part of the large-sized crystal grains was cut from the sheet, and the crystal orientations were measured by an X-ray diffraction method. The

\* Corresponding author at: R&D Center, Sumitomo Light Metal Industries, Ltd., 3-1-12 Chitose, Minato-ku, Nagoya, Aichi 455-8670, Japan. Tel.: +81 52 651 2103; fax: +81 52 651 8117.

E-mail address: [shingo.ikawa@mail.sumitomo-lm.co.jp](mailto:shingo.ikawa@mail.sumitomo-lm.co.jp) (S. Ikawa).

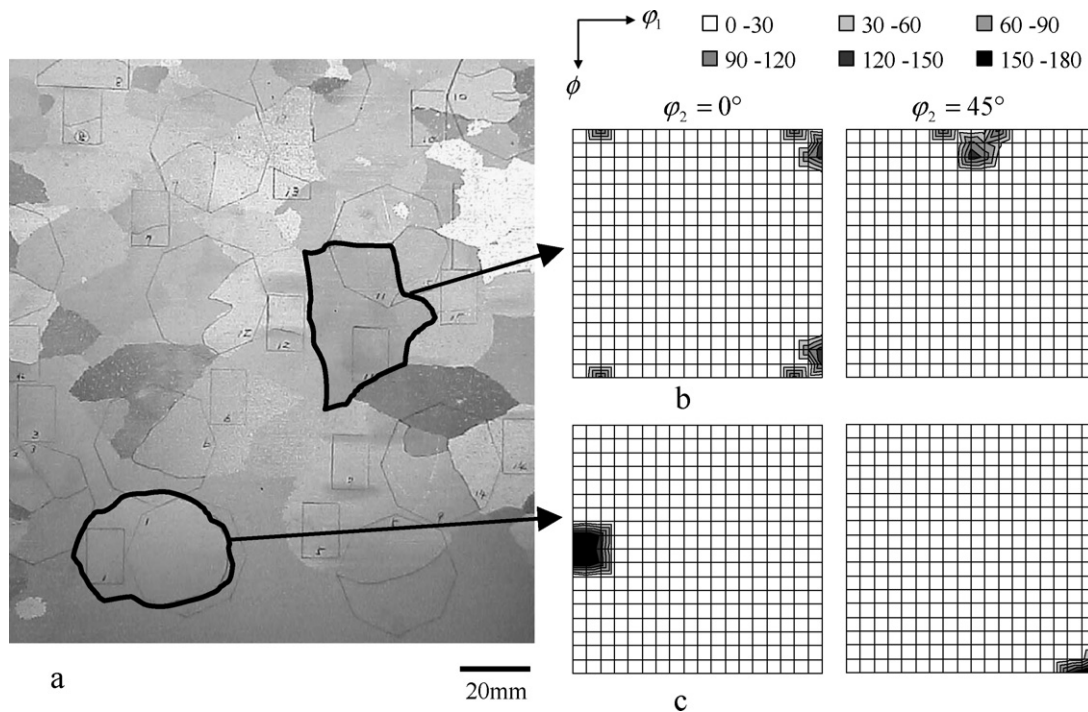


Fig. 1. (a) Micrographs for surface of Al-Mg-Si alloy sheet; ODFs for grains oriented in almost cube orientation (b) and Goss orientation (c).

crystal grains enclosed by the thick lines in Fig. 1(a) were oriented in the cube and Goss orientations, respectively, as shown in Fig. 1(b) and (c). The bending specimens of 15 mm × 35 mm were cut from these crystal grains. In the present study, these will be called the cube and Goss specimens, respectively. We observed the distributions of second phase particles, and confirmed that the number of particles whose sizes were larger than 2 μm was almost equal in both grains.

The so-called 180° bending test method specified in ISO7438 (JIS Z 2248) was performed. Fig. 2 shows the procedure of the test. A rectangular specimen is firstly bent by means of the three point bending method, in which the punch has a radius of curvature of 0.5 mm. Then, the specimen is pressed so that the both sides of specimen contact with each other. The total thickness of the final hems is approximately twice the thickness of the sheets.

The bending tests were basically carried out in three directions of  $\Phi = 0^\circ$ ,  $45^\circ$ , and  $90^\circ$ , where  $\Phi$  is an angle relative to the rolling direction (RD) and measured counterclockwise in the sheet plane as shown in Fig. 2. In case of the cube, the bending orientations of  $\Phi = 0^\circ$  and  $90^\circ$  are crystallographically equivalent. Hence, only the test for  $\Phi = 0^\circ$  was done.

## 2.2. Results

Fig. 3 shows the optical micrographs of cross-sections at the center of the specimen width after testing. In the case of the cube, the specimens were smoothly bent without any surface waviness and no breakage occurred both for  $\Phi = 0^\circ$  and  $45^\circ$  (Fig. 3(a) and (b)). In the cube specimen at  $\Phi = 45^\circ$  (Fig. 3(b)), many narrow slip bands (micro-slip bands) are seen, but they seem to be uniformly distributed near the sheet surface and no concentration of them is observed. The Goss specimen at  $\Phi = 0^\circ$  was also bent rather smoothly, but a surface waviness with a small amplitude is seen (Fig. 3(c)). Weak concentrations of micro-slip bands from valleys of the wave into the inner region are observed. In contrast, the Goss specimen at  $\Phi = 45^\circ$  exhibited clear concentrations of the micro-slip bands in the form of wider cross-shaped bands (two of

those are visible in the micrograph, Fig. 3(d)). In the present paper, this type of concentration of the micro-slip bands is referred to as the macroscopic shear band (macro-shear band). A break along the macro-shear band is observed for the Goss at  $\Phi = 45^\circ$ . The break is more pronounced for the Goss specimen at  $\Phi = 90^\circ$  (Fig. 3(e)).

## 3. Finite element analysis

### 3.1. Constitutive equations and problem formulation

It is assumed here that the most severely bent region in the specimens of the pushing–bending tests was subjected to a pure bending. In the present numerical investigation, we perform finite element analyses of the pure bending problem, employing the crystal plasticity constitutive model presented by Asaro [6] and Peirce et al. [7].

In the crystal plasticity model, the slip rate on the  $\alpha$ th slip system is assumed to be given by the following power law relation:

$$\dot{\gamma}^{(\alpha)} = \dot{\gamma}_0 \operatorname{sgn}(\tau^{(\alpha)}) \left| \frac{\tau^{(\alpha)}}{g^{(\alpha)}} \right|^{1/m}, \quad (1)$$

where  $\dot{\gamma}_0$  is the reference slip rate,  $\tau^{(\alpha)}$  is the resolved shear stress,  $m$  is the rate sensitivity exponent and  $g^{(\alpha)}$  is the hardness of the slip system. The evolution law for  $g^{(\alpha)}$  is given by

$$\dot{g}^{(\alpha)} = h \sum_{\beta} |\dot{\gamma}^{(\beta)}|, \quad h = h_0 \left( 1 + \frac{h_0 \gamma_a}{\tau_0 n} \right)^{n-1}, \quad \gamma_a = \int_0^t \sum_{\alpha} |\dot{\gamma}^{(\alpha)}| dt, \quad (2)$$

where  $\tau_0$  is the initial value of  $g^{(\alpha)}$ ,  $h_0$  is the initial slip hardening modulus,  $n$  is a power law hardening exponent, and  $t$  is the time.

Fig. 4 shows a schematic illustration of the pure bending problem. The formulation and the boundary conditions for the pure bending problem are the same as those used by one of the authors [4]. Here,  $T_0$  and  $L_0$  are defined, respectively, as the thickness and the length of the initial configuration of a rectangular part of the sheet. The pure bending is a simplification of the deformation mode

Download English Version:

<https://daneshyari.com/en/article/1579200>

Download Persian Version:

<https://daneshyari.com/article/1579200>

[Daneshyari.com](https://daneshyari.com)